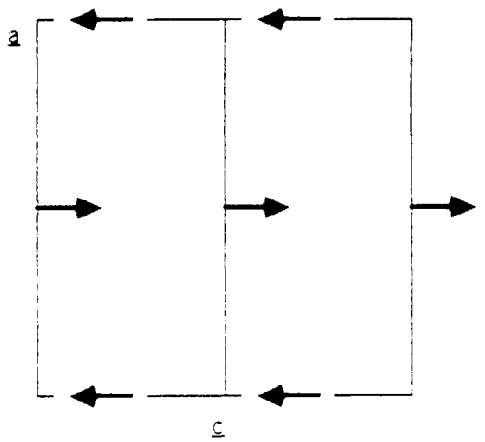

Figure 6. Schematic representation of the preferred spin orientation for I in the *ac* plane. The arrows indicate the manganese spins; those of the copper ions would be in the opposite directions.

Alternative explanations, which attribute the shifts to intrinsic g variations due to selective thermal population of different spin states, do not appear to be relevant here, because in no way could they give both positive and negative deviations from the high-temperature value.

The resonance fields along the three principal axes can be expressed as[28]

$$B_a = \left(\sqrt{\chi_b \chi_c}/\chi_a\right)(g_e/g_a)B_0 \qquad (4)$$

where χ_a, χ_b, and χ_c are the principal susceptibilities in the paramagnetic region, g_a is the indicated principal g value, $g_e = 2.0023$, and B_0 is the resonance field of the free electron. The resonance fields for the other crystal directions follow from cyclic permutations.

The observed shifts compare well with the reported magnetic anisotropy data, which showed that $\chi_c > \chi_a > \chi_b$ for I and $\chi_c > \chi_a > \chi_b$ for II. The high value observed for χ_c has been attributed to anisotropic exchange that tends to align the spins orthogonal to *a*. The present EPR data at high temperature suggest that the main dipolar interaction must be parallel to *c*, and if we assume that it dominates the interchain interaction, we must conclude that the spins are parallel to each other along this direction. Therefore, an alternative spin distribution for I may be suggested, as compared to ref 19, where the spins were assumed to be oriented by an interchain antiferromagnetic exchange interaction. The suggested spin alignment is shown in Figure 6. Such a spin structure agrees with the weak ferromagnetism observed[20] for I along *a* because the antiferromagnetically coupled manganese(II) ions occupy magnetically nonequivalent sites. In this particular case, where the manganese ion lies in a special position, only canting in the *ac* plane is possible, yielding weak ferromagnetism along *a*. The suggested structure seems to be the only one compatible with magnetic symmetry requirements.[31] The difference between I and II lies mainly in the coupling in the planes orthogonal to *c*: for I this yields alternate planes with antiparallel spin alignment, while for II all the spins are parallel. The nearest-neighbor interactions along *c* are parallel in both cases.

Acknowledgment. This work was financially supported by NATO Research Grant 0271/83 and by Stimulation Contract ST2J-0218-1-F(eds) from the European Economic Community.

Registry No. I, 101935-07-3; II, 105121-18-4.

(31) Opechowsky, W.; Guccione, R. In *Magnetism*; Rado, G. T., Suhl, H., Eds.; Academic Press: New York, 1963.

Contribution from the Chemistry Department, University of Virginia, Charlottesville, Virginia 22901

Matrix Infrared Spectra of Reaction and Photolysis Products of Stibine and Ozone

Lester Andrews,* Brian W. Moores,[1] and Kathleen K. Fonda

Received July 6, 1988

Argon-diluted samples of stibine and ozone were codeposited at 12 K and examined by infrared spectroscopy. Isotopic substitution (SbH_3, SbD_3, $^{16}O_3$, $^{18}O_3$, $^{16,18}O_3$) provided a basis for identification of the major reaction products as stibylene ozonide, $HSbO_3$, and hydroxystibine, H_2SbOH. Red photolysis produced new bands identified as stibine oxide, H_3SbO, and ultraviolet photolysis destroyed $HSbO_3$, decreased H_3SbO, increased H_2SbOH, and produced weak bands probably due to $HOSbO_2$.

Introduction

As part of a program involving the study of new reactive molecular species trapped in low-temperature matrices, we have recently investigated the infrared spectra of mixtures of ozone in solid argon with the group 15 hydrides ammonia,[2] phosphine,[3,4] and arsine.[5] These studies have identified several new species formed when the mixtures were irradiated with visible or ultraviolet light. In all of these cases, there is evidence for the formation of a stable complex between the precursor ozone and hydride submolecules, and reaction occurs following red photolysis of the molecular complex, which does not photolyze ozone isolated in solid argon. First, the ozone submolecule in the complex undergoes photodissociation, and the photolytically generated oxygen atom then adds to the hydride submolecule within the complex. In the case of phosphine and arsine, a substantial yield of photoproducts was formed when irradiation was carried out by using red light.[4,5] Since the cross section for absorption of 600-nm photons by isolated ozone molecules is smaller by a factor of 10^5 than that for 250-nm photons,[6] the complex appears to have a much higher probability for red photodissociation than does isolated ozone.

In the ammonia–ozone and phosphine–ozone reactions, no evidence for reaction between the precursor molecules was found during codeposition before photolysis. In the case of arsine and ozone, however, reaction products were formed during codeposition of the samples. We have carried out a study of the stibine–ozone system, motivated by a desire to complete a systematic investigation of the matrix reaction of group 15 hydrides with ozone and to discover possible periodic trends in their reactivity and photochemistry. A further motivation for this work was the relative

* To whom correspondence should be addressed.

(1) On sabbatical leave from Randolph-Macon College, Ashland, VA 23005.
(2) Withnall, R.; Andrews, L. *J. Phys. Chem.* **1988**, *92*, 2155.
(3) Withnall, R.; Hawkins, M.; Andrews, L. *J. Phys. Chem.* **1986**, *90*, 575.
(4) Withnall, R.; Andrews, L. *J. Phys. Chem.* **1987**, *91*, 784.
(5) Andrews, L.; Withnall, R.; Moores, B. W. *J. Phys. Chem.*, in press.
(6) Baulch, D. L.; Coty, R. A.; Crutzen, R. J.; Hampson, R. F.; Kerr, J. A.; Troe, J.; Watson, R. T. *J. Phys. Chem. Ref. Data* **1982**, *11*, 327.

0020-1669/89/1328-0290$01.50/0

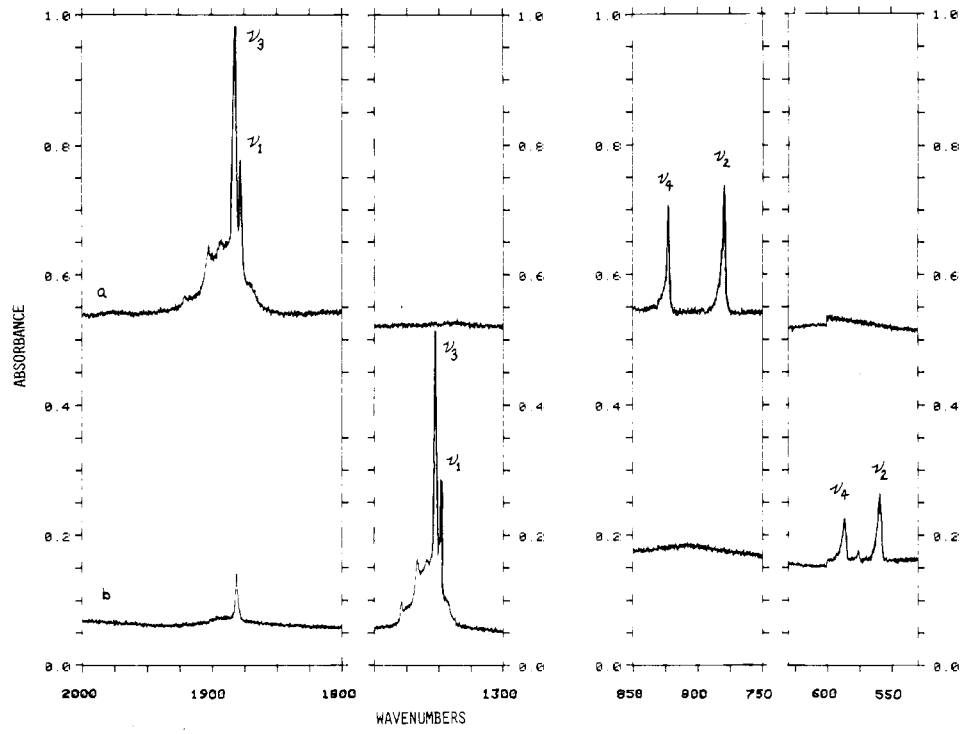

Figure 1. Infrared spectra in the fundamental regions for $Ar/SbH_3 = 200/1$ samples (2 mmol) at 12 K: (a) SbH_3; (b) SbD_3.

sparseness of spectroscopic or structural data on small antimony-containing molecules, in particular the lower oxyacids, where more is known in the case of arsenic[7,8] than that of antimony,[9] and also the higher (V) oxidation state species of antimony.

Experimental Section

The refrigeration system, vacuum chamber, and experimental technique for preparing and depositing matrix samples and carrying out photolyses have been described previously.[2-5,10] In these experiments high-pressure mercury-arc photolyses were done by using wavelengths in the 590–1000-, 290–1000- and 220–1000-nm regions. In the photolysis Corning glass filters were used in conjunction with a 10-cm water filter. Infrared spectra were recorded on a Perkin-Elmer 983 spectrophotometer and data system at 4-cm^{-1} resolution and, in regions of interest, at 1-cm^{-1} resolution. Sharp bands reported to 0.1 cm^{-1} are accurate to ± 0.3 cm^{-1}, and bands reported to 1 cm^{-1} are accurate to ± 1 cm^{-1}.

Samples of ozone were made, with either $^{16}O_2$ to prepare $^{16}O_3$, $^{18}O_2$ to prepare $^{18}O_3$, or a mixture of isotopes to prepare isotopically "scrambled" ozone, were purified, and were diluted with argon as described previously.[11] The mixtures employed here were Ar/O_3 in 100/1 or 300/1 mole ratios.

Stibene was prepared and purified by following the method of Jolly and Drake.[12] In the case of stibine-d_3 the analogous reaction was carried out in a deuteriated environment: water-d_2 was used as the solvent, sulfuric acid was replaced with sulfuric acid-d_2, and potassium tetrahydroborate-d_4 was used as the reducing agent. Isotopic purities of the water-d_2 and potassium tetrahydroborate-d_4 were better than 99%; that of the sulfuric acid-d_2 was 98%. On the basis of spectra to be discussed later, the stibine-d_3 product is estimated to be better than 90% isotopically pure. The stibines were stored in Pyrex vessels under liquid nitrogen, and under these conditions no decomposition was apparent even after 6 weeks. Mixtures of argon and stibine ($Ar/SbH_3 = 200/1$) were freshly prepared in a 3-L stainless steel can for each matrix experiment. On the basis of the intensity of stibine infrared bands in a matrix made from a leftover sample, the half-life of stibine in the argon mixture at room temperature was approximately 2 days. Mixtures were prepared by removing the liquid-nitrogen bath from the stibine storage vessel, opening the valve to the vacuum manifold, and allowing the vessel to warm until the desired pressure of stibine vapor was reached in the vacuum manifold. The valve to the storage vessel was closed while the liquid-nitrogen bath was simultaneously replaced, and stibine vapor in the manifold was expanded into the 3-L can and diluted with argon.

In most experiments Ar/SbH_3 and Ar/O_3 mixtures were codeposited from separate spray-on lines, spectra were taken of the unphotolyzed deposit, and then photolyses were carried out at successively shorter wavelengths. In some experiments only a small amount of Ar/SbH_3 or Ar/SbD_3 was deposited, in order to record the fundamental vibrational frequencies of the stibines in solid argon or to photolyze this sample alone.

Table I. Comparison of Stibine Infrared Absorptions (cm^{-1}) in Solid Argon at 12 K and in the Gas Phase

solid argon[a]		gas phase[b]		
SbH_3	SbD_3	SbH_3	SbD_3	assgnt
1877.8	1348.4	1891	1359	ν_1, sym str
779.2	559.1	782	561	ν_2, sym bend
1882.2[c]	1352.7[d]	1894	1362	ν_3, antisym str
822.4	586.2	831	593	ν_4, antisym bend
3695.0	2669.2			$2\nu_3$, overtone

[a] In addition, Sb–H isotopic impurity was observed at 1880.7 cm^{-1}, and bending modes were observed at 717.7 and 692.1 cm^{-1}, which are probably due to $SbHD_2$. [b] Reference 13. [c] Sharp weak bands at 1921, 1902, and 796 cm^{-1} are believed due to repulsive matrix sites. [d] Sharp weak bands at 1378, 1366, and 576 cm^{-1} are believed due to repulsive matrix sites.

Results

Argon matrix experiments with isotopic stibine and ozone reagents will be described in turn.

Stibine. Argon/stibine samples were examined with 2 mmol deposited, which gave good measurements of the sharp fundamentals that are shown in Figure 1 and listed in Table I. Comparison with gas-phase band-center measurements[13] reveals 3–13-cm^{-1} red shifts due to interaction with the matrix. A thicker sample (10–11 mmol) gave completely absorbing fundamentals, a sharp 3695-cm^{-1} $2\nu_3$ band, and traces of water and CO_2 im-

(7) Bailar, J. C.; Emeleus, H. J.; Nyholm, R.; Trotman-Dickenson, A. F. *Comprehensive Inorganic Chemistry*; Pergamon Press: Oxford, England, 1973; Vol. 2, pp 635–636.
(8) Cavell, R. G.; Sanger, A. R. *MTP International Review of Science: Inorganic Chemistry, Series One*; Butterworths: London, 1972; Vol. 2, p 203.
(9) Moss, K. C.; Smith, M. A. R. *MTP International Review of Science: Inorganic Chemistry, Series Two*; Butterworths: London, 1975; Vol. 2, p 221.
(10) Moores, B. W.; Andrews, L. *J. Phys. Chem.*, in press.
(11) Andrews, L.; Spiker, R. C., Jr. *J. Phys. Chem.* **1972**, *76*, 3208.
(12) Jolly, W. C.; Drake, J. E. *Inorg. Synth.* **1963**, *7*, 34.
(13) Haynie, W. H.; Nielsen, H. H. *J. Chem. Phys.* **1953**, *21*, 1839.

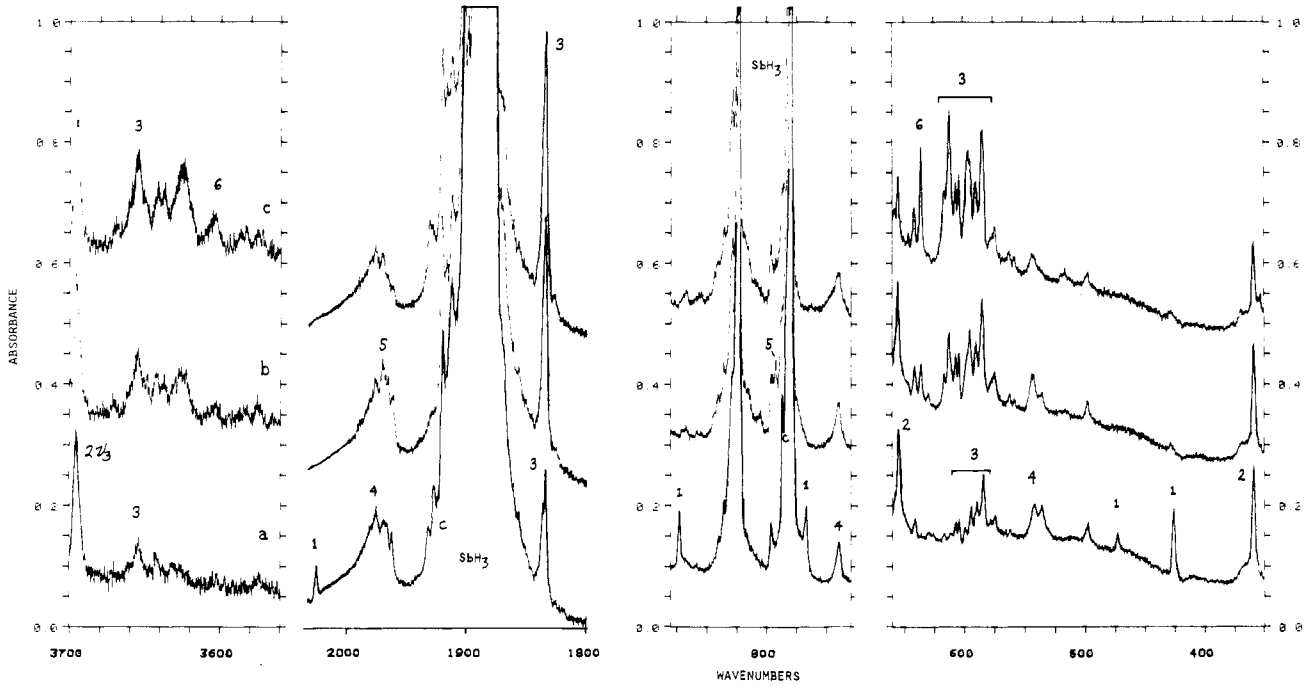

Figure 2. Infrared spectra for Ar/SbH_3 = 200/1 (13 mmol) and Ar/O_3 = 100/1 (9 mmol) mixtures: (a) after codeposition at 15 K for 3.5 h; (b) after 290–1000-nm photolysis for 30 min; (c) after 220–1000-nm photolysis for 30 min.

purities. This samples was subjected to 290–1000-nm photolysis for 30 min, and no changes were observed in the spectrum; however, 220–1000-nm irradiation for 30 min produced a new 1840.5-cm^{-1} absorption (A = absorbance = 0.05) and decreased precursor absorptions slightly. A similar treatment was done for SbD_3 samples; a sharp band at 1880.7 cm^{-1}, intermediate between ν_1 and ν_3 for SbH_3, is probably due to the Sb–H stretching mode for $SbHD_2$, and sharp 717.7- and 692.1-cm^{-1} bands are due to bending modes for the mixed isotopic molecule $SbHD_2$; the latter bands are in reasonable agreement with calculated fundamentals for deuteriated stibines.[14] The observation of only one sharp band in the 1800-cm^{-1} region suggests that no detectable SbH_2D and SbH_3 isotopic impurities were present. A thicker Ar/SbD_3 sample was photolyzed by 290–1000-nm irradiation to no avail, but 220–1000-nm irradiation for 30 min produced a new 1320.2-cm^{-1} band (A = 0.13) with a 1318-cm^{-1} shoulder and again slightly decreased precursor absorptions. Sample warming to 30 K for 5 min decreased the 1320-cm^{-1} band (to A = 0.09) and destroyed the 1318-cm^{-1} shoulder without changing SbD_3 absorptions. A final annealing to 36 K virtually destroyed the 1320-cm^{-1} band with little effect on SbD_3 bands.

SbH_3 and Ozone. A series of 14 matrix experiments was performed with stibine and ozone under different codeposition and photolysis conditions. The samples were faint brown, and elemental antimony remaining on the window caused formation of a scattering matrix in the subsequent experiment unless the window was carefully cleaned. Figure 2 shows representative spectra, and Table II lists the product absorptions and characterizes them according to production by reaction during codeposition (R) or photolysis (P) of reagents. Precursor complex absorptions noted C include a weak doublet on the blue side of the precursor stretching absorption, a red ozone ν_3 satellite, and a blue SbH_3 ν_2 satellite; these bands decreased markedly on photolysis. Other reaction product absorptions can be grouped into four sets of bands on the basis of photolysis behavior: group 1, bands unchanged on 590- or 520-nm photolysis, half destroyed by 420–1000-nm radiation, and destroyed by 290-nm photolysis; group 2, bands unchanged on visible or 290-nm photolysis but half destroyed by 220–1000-nm radiation; group 3, bands showing little growth on 290-nm irradiation, and another 15% growth on

Table II. Absorptions (cm^{-1}) Observed in Argon Matrix Experiments with Stibine and Ozone

$^{16}O_3$	$^{18}O_3$	characteristic[a]	identification[b]
3654	3643	R, +g	3
3640	3626	R, +g	3
3625	3614	R, +g	3
3604	3593	P, +u	6
3575		P, +u	6
2027	2027	R, -u	1
1982	1982	R, -	4
1970	1970	P, +r, -u	5
1932	1932	R, -r	C
1927	1927	R, -r	C
1836.8	1837.0	R, +g	3
1834.6	1834.5	R, +g	3
1291	1284	R, +	?
1032.0	976.2	R, -r	C
918	918	R, +	?
872.7	871.6	R, -u	1
791.8	794.2	P, +r, -u	5
786.7	786.7	R, -r	C
767.4	755.6	R, -u	1
740	713	R, -u	4
654.9	641.1	R, -u	2
640.9	610.2	R, +u	6?
635	604	P, +u	6
612	582	R, +u	3
596	567	R, +g	3
584	556	R, +g	3
574	548	R, +g	3
542	516	R, -u	4
494		R, +u	?
472	473	R, -u	1
426	408	R, -u	1
370	369	P, +u	6
358	355	R, -u	2

[a] Symbols: R = reaction product and P = photolysis product. Photolysis behavior is indicated by growth (+ = increase, - = decrease) and range (r = red, g = green, u = ultraviolet). [b] Absorption groups identified in text.

(14) Whitmer, J. C. *J. Chem. Phys.* **1972**, *56*, 1050.

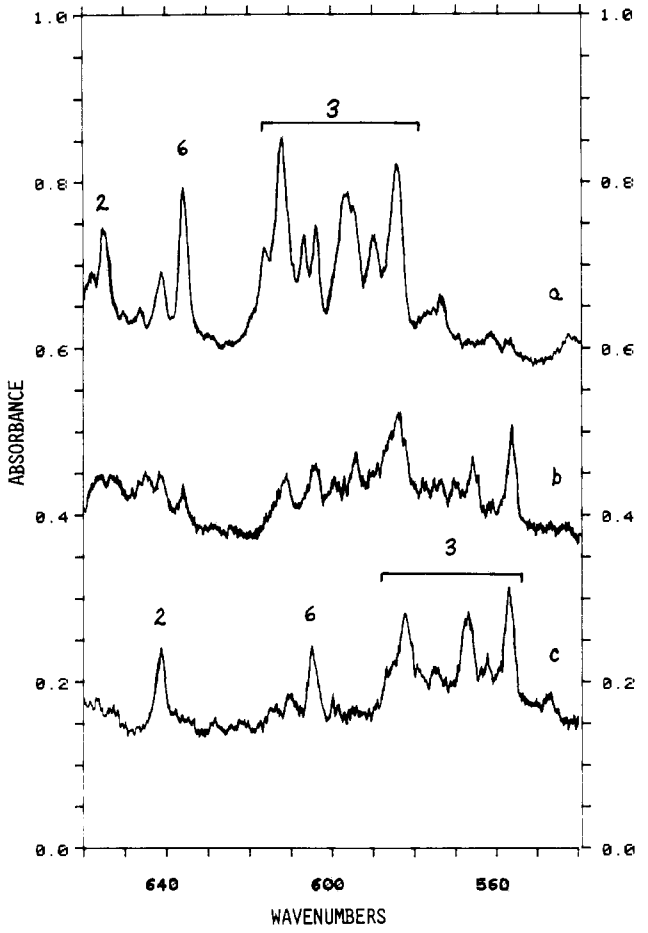

Figure 3. Infrared spectra in the 540–660-cm^{-1} region for Ar/SbH_3 = 200/1 samples codeposited with Ar/O_3 = 100/1 samples after 220–1000-nm photolysis for 30 min: (a) $^{16}O_3$; (b) $^{16,18}O_3$; (c) $^{18}O_3$.

220–1000-nm photolysis; group 4, reaction-product bands that show little change on photolysis. Finally, two sets of bands for new photolysis products appeared: group 5, bands produced with 630-, 590-, or 520-nm radiation, increased slightly with 290-nm photolysis, and decreased by 220–1000-nm light; group 6, bands produced on 290-nm photolysis and doubled on 220–1000-nm irradiation.

Several experiments were performed with SbH_3 and $^{18}O_3$, and the oxygen-18 counterpart absorptions are listed in Table II. Figure 3 contrasts the spectrum after full arc photolysis with $^{18}O_3$ and $^{16}O_3$ in the region of largest isotopic effect. A clear isotopic dependence was also found in the 3600-cm^{-1} region. Two studies were done with a mixed isotopic $^{16,18}O_3$ sample. In most spectral regions (i.e. 540–640 cm^{-1} in Figure 3b) the mixed isotopic spectrum consisted of the superposition of $^{16}O_3$ and $^{18}O_3$ spectra. However, the 655-cm^{-1} band became a doublet of doublets (655, 652, 645, 641 cm^{-1} in Figure 3b), the 767-cm^{-1} band exhibited a triplet of doublets with more intense intermediate components at 760 and 761 cm^{-1}, and the 426-cm^{-1} band revealed a partially resolved multiplet with two more intense intermediate components at 419 and 413 cm^{-1}.

SbD_3 and Ozone. Eight studies were done with SbD_3 and ozone. Figure 4 illustrates spectra analogous to those of Figure 2, and Table III gives the product positions. The most obvious difference between SbD_3 and SbH_3 is the *lesser reactivity* of SbD_3 on co-deposition with ozone. In particular, group 3 bands were strong in SbH_3 experiments (Figure 2a) and virtually absent in SbD_3 studies (Figure 4a) and no evidence was found for group 2 bands with SbD_3. However, the group 1 absorptions were more prominant with SbD_3 than with SbH_3.

Photolysis with red light (590–1000 nm) reduced precursor complex bands (noted C) and increased group 3 bands (1320 cm^{-1} from $A < 0.01$ to $A = 0.02$) and the group 5 bands (824.6 cm^{-1} from $A = 0.02$ to 0.18), while group 1 bands were not changed (spectrum not shown in Figure 4). Continued irradiation at 290 nm, shown in Figure 4b, produced major growth in group 3 (5-fold) and group 5 (2-fold) bands, while group 1 bands were destroyed, and further 220-nm photolysis doubled group 3 bands and reduced group 5 absorptions by 30%.

Two experiments were done with SbD_3 and $^{18}O_3$, and the oxygen-18 counterpart absorptions are given in Table III. Figure 5 shows oxygen isotopic spectra for three group 1 bands, and the

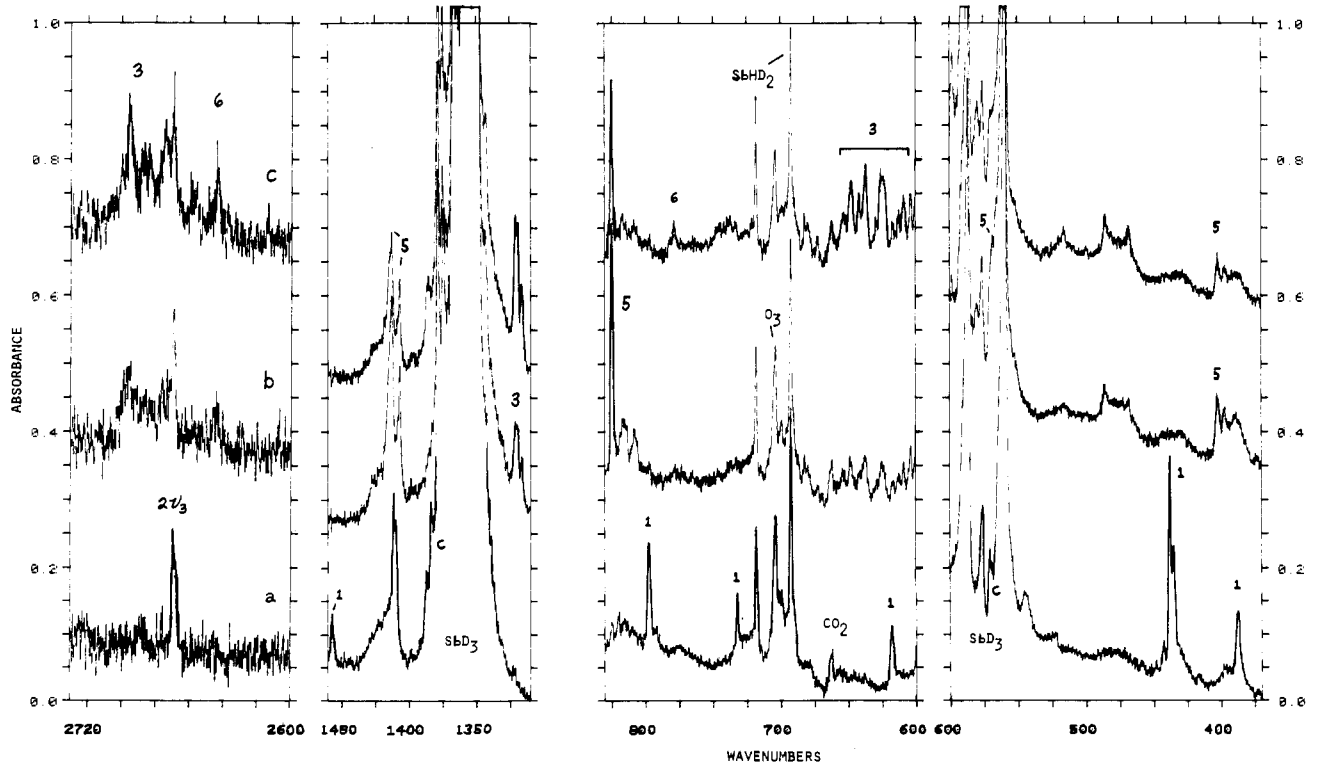

Figure 4. Infrared spectra for Ar/SbD_3 = 200/1 (16 mmol) and Ar/O_3 = 100/1 (11 mmol) mixtures (a) after codeposition for 4 h at 15 K; (b) after 290–1000-nm photolysis for 30 min; (c) after 220–1000-nm photolysis for 30 min.

Table III. Absorptions (cm^{-1}) Observed in Argon Matrix Experiments with SbD_3 and Ozone

$^{16}O_3$	$^{18}O_3$	characteristic[a]	identification[b]
2697	2680	P, +g	3
2686		P, +g	3
2674	2657	P, +g	3
2658	2642	P, +u	6
2644	2627	P, +u	6
1457.7	1456.7	R, -u	1
1413	1413	P, +r	5
1411	1411	R, -	4
1407	1407	P, +r	5
1387	1387	R, -r	C
1384	1387	R, -r	C
1320.6	1320.6	R, +g	3
1319.4	1319.4	P, +g	3
1316.3	1316.3	P, +g	3 site
1032	976	R, -r	C
824.6	781.0[c]	P, +r, -u	5
796.7	754.2	P, -u	1
778.5	736.5	P, +u	6
732		R, -	?
647	613	P, +u	3
641		P, +u	3
637	609	P, +u	3
624	603	P, +u	3
617.6	615.6	P, -u	1
608	580	P, +u	3
603	*d*	P, +u	3 site
598	*d*	P, +u	3
580	*d*	P, +u	3 site
569.9	569.9	R, -r	C
568	568	P, +r, -u	5
485	468	P, +u	?
437.9	426.0	R, -u	1
435.0	423.5	R, -u	1 site
402.0	399.4	P, +u	5
396.6	394.1	P, +r, -u	5
387.1	381.0	R, -u	1
276	272	P, +u	6

[a] Symbols: R = reaction product and P = photolysis product. Photolysis behavior is indicated by growth (+ = increase, - = decrease) and range (r = red, g = green, u = ultraviolet). [b] Absorption groups identified in text. [c] Weak band also observed at 795 cm^{-1}. [d] Obscured by precursor.

intermediate trace b from one of two $^{16,18}O_3$ experiments shows the mixed isotopic multiplets for these bands. The upper region shows five bands at 796.7, 787.6, 775.6, 765.2, and 754.2 cm^{-1}, and the lower region reveals a partially resolved sextet measured at 437.9, 434.8, 432.2, 429.0, 426.2, and 423.6 cm^{-1} under best resolution conditions and an unresolved multiplet between 387 and 381 cm^{-1}. The 2600- and 600-cm^{-1} regions showed oxygen-18 shifts and no evidence of multiplets with mixed isotopic ozone. The sharp red-photolysis-product band at 824.6 cm^{-1} with $^{16}O_3$ shifts to 781.0 cm^{-1} with $^{18}O_3$; the latter band was produced by 630–1000-nm photolysis; 520–1000-nm radiation gave no more, but 290–1000-nm light tripled the band (to $A = 0.08$), and a weak associated band appeared at 795.3 cm^{-1}. With $^{16,18}O_3$, the sharp 824.6- and 781.0-cm^{-1} group 5 bands exhibited no splittings or mixed isotopic components. Finally, the ozone region was examined and the photosensitive satellite sextet at 1032, 1018, 1009, 999, 985, and 975 cm^{-1} exhibited 1/2/1/1/2/1 relative intensities just as ν_3 of O_3.

Complementary experiments were done with $Ar/O_2 = 50/1$ samples passed through a microwave discharge and codeposited with $Ar/SbD_3 = 200/1$ samples. A strong 1319.6-cm^{-1} band ($A = 0.21$) was observed along with weak, broad 600–650- and 2696–2685-cm^{-1} absorptions, about 20% of the absorbance of the bands found in Figure 4c, where the 1320-cm^{-1} band absorbance is 0.20. Weak ozone absorptions were also observed, and no group 1 or group 5 band were detected. When only argon was passed through the microwave discharge and the vacuum ultraviolet radiation directed at the condensing sample, no new product absorptions were observed.

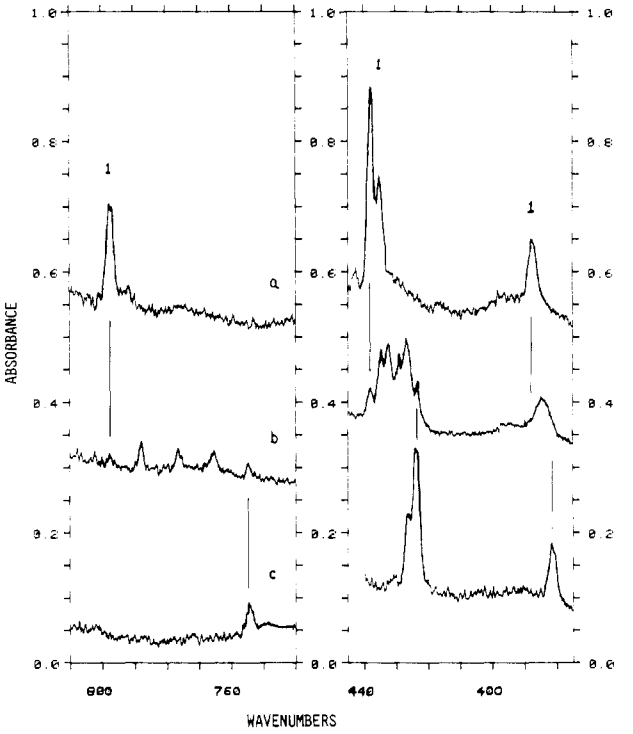

Figure 5. Infrared spectra in the 740–810- and 370–450-cm^{-1} regions for $Ar/SbD_3 = 200/1$ samples codeposited at 15 K with $Ar/O_3 = 100/1$ samples: (a) $^{16}O_3$; (b) $^{16,18}O_3$; (c) $^{18}O_3$.

Discussion

The new products will be identified, absorptions will be assigned, and reactivity trends for group 15 hydrides with ozone will be considered.

Stibino Radical. Since the first absorption of SbH_3 is a broad continuum with a maximum at 197 nm[15] and 193-nm ArF laser radiation photodissociates SbH_3 to give SbH_2,[16] it is reasonable to expect full high-pressure mercury-arc photolysis, which gives significant radiation between 220 and 250 nm, to photolyze SbH_3 (reaction 1). The new 1840.5-cm^{-1} band produced at the expense

$$SbH_3 + h\nu\ (220\text{–}250\ nm) \rightarrow SbH_2 + H \qquad (1)$$

of SbH_3 by such photolysis is assigned to ν_3 of the stibino radical SbH_2. Although the ground-state SbH diatomic fundamental has not been observed experimentally, it has recently been calculated[17] at 1763 cm^{-1}, sufficiently far below 1840 cm^{-1} to rule out assignment to SbH. It is interesting to note that the fundamentals for the transient species SbH_2 and SbH fall below SbH_3. This suggests that extra repulsions from the unpaired electron(s) adversely affect the remaining bond(s). Similarly, the 1320.2-cm^{-1} band produced at the expense of SbD_3 is assigned to ν_3 of the SbD_2 radical. Sample annealing verified the transient nature of the new species absorbing at 1320 cm^{-1}. Finally, the microwave-discharge O atom reaction with SbD_3 also produced a significant yield of the 1320-cm^{-1} SbD_2 absorption. On the basis of the observation of other bands to be assigned below to D_2SbOD, the abstraction reaction for O appears to be favored over insertion or addition and rearrangement.

Stibylene Ozonide (Group 1). Table IV lists the group 1 bands that are produced on codeposition of stibine and ozone with excess argon. The photodissociation profile, i.e., photolysis behavior, indicates blue near-UV absorption, similar to that observed for alkali-metal and alkaline-earth-metal ozonides.[18,19] The group 1 bands contain an Sb–H stretching fundamental at 2027 cm^{-1},

(15) Humphries, C. M.; Walsh, A. D.; Warsop, P. A. *Discuss. Faraday Soc.* **1963**, *35*, 148.
(16) Ni, T.; Yu, S.; Ma, X.; Kong, F. Chem. *Phys. Lett.* **1986**, *128*, 270.
(17) Balasubramanian, K.; Tanpipat, N.; Bloor, J. E. *J. Mol. Spectrosc.* **1987**, *124*, 458.
(18) Andrews, L. *J. Chem. Phys.* **1975**, *63*, 4465.
(19) Ault, B. S.; Andrews, L. *J. Mol. Spectrosc.* **1977**, *65*, 437.

Table IV. Infrared Absorptions (cm^{-1}) Assigned to Stibylene Ozonide in Solid Argon

$HSb^{16}O_3$	$HSb^{18}O_3$	$DSb^{16}O_3$	$DSb^{18}O_3$	mode
2027	2027	1457	1457	Sb–H str
872.7	871.6	617.6	616.0	antisym Sb–H def[a]
767.4	755.6	796.7	754.2	antisym O–O str[a]
727	686	731.8	(690)[b]	$Sb–O_3$ str
472.4	473	387	381	sym Sb–H def[a]
425.6	407.7	437.9	423.6	sym O–O–O bend[a]
				sym Sb–O str[a]

[a] Denotes mixed internal coordinates for normal modes. [b] Estimated from the position of one double-intensity intermediate component at 711.3 cm^{-1} for the 731.9-cm^{-1} band; obscured by the strong 692-cm^{-1} precursor band.

above that for SbH_3, with an appropriate H/D = 2027/1457 = 1.3912 ratio and an Sb–H deformation fundamental at 872.7 cm^{-1}, also above that for SbH_3, with a large H/D = 872.7/617.6 = 1.413 ratio and a small (1.1 cm^{-1}) oxygen-18 shift arising from interaction with a nearby stretching mode involving oxygen. Two other bands, 767.4 and 425.6 cm^{-1}, show large oxygen isotopic shifts and multiplets with $^{16,18}O_3$ indicative of a three oxygen atom species. The final band at 472.4 cm^{-1} is essentially unchanged with oxygen-18 and shows the moderate H/D = 472.4/387 = 1.221 ratio expected for a symmetric deformation mode. That the two oxygen stretching motions interact with the two Sb–H deformation modes is clearly revealed in the spectrum of the deuteriated species, where the two primarily oxygen motions *blue shift* owing to the large red shifts and crossover of the corresponding Sb–D deformation modes.

The diagnostic group 1 bands are illustrated in Figure 5 for isotopic ozone precursors. The 796.7-cm^{-1} band exhibits a doublet of 1/2/1 triplets with the two central components almost coincident; this multiplet is reminiscent of ozonide spectra[20] and indicates a vibration of two equivalent oxygen atoms and one inequivalent oxygen atom. In fact, the band position (796.7 cm^{-1}) is in agreement with $M^+O_3^-$ values for the antisymmetric O–O stretching motion of the ozonide anion (800 ± 10 cm^{-1}).[20] The 437.9-cm^{-1} band exhibits a 1/2/1/1/2/1 relative intensity sextet again showing three oxygen atoms with two of them equivalent. Thus, species 1 has one Sb–H subunit, as evidenced by one stretching and two widely separated deformation modes, and one O_3 subgroup, as evidenced by two stretching modes, and the $HSbO_3$ identification is straightforward. Stibylene ozonide is probably a pyramidal molecule with a plane of symmetry produced by direct reaction (eq 2) of the precursor molecules.

$$SbH_3 + O_3 \longrightarrow H—\ddot{S}b\begin{matrix}O\\ |\\ O—O\end{matrix} + H_2 \qquad (2)$$

The vibrational assignments for $HSbO_3$ are interesting because of different amounts of mode mixing for the different isotopic species. The purest mode, 796.7 cm^{-1} for $DSb^{16}O_3$, is primarily antisymmetric O–O–O stretching from near agreement with $M^+O_3^-$ values[20] and oxygen-18 shift (751.1 cm^{-1} calculated for a pure oxygen motion as compared to the 754.2-cm^{-1} observed value). This motion involves even more oxygen character than an Sb–O stretching mode (calculated ^{18}O value 756.5 cm^{-1}). The antisymmetric Sb–D deformation mode at 617.6 cm^{-1} is low enough to interact little and have little effect on the O_3-subgroup character of the 796.7-cm^{-1} normal mode. However, with $HSbO_3$, the antisymmetric Sb–H deformation mode at 872.7 cm^{-1} interacts with the O_3-subgroup mode, forces it down to 767.4 cm^{-1}, and reduces the oxygen character of this mode. A similar interaction operates between the symmetric Sb–H deformation at 472.4 cm^{-1} and mixed Sb–O stretch, O–O–O bend at 425.6 cm^{-1}. The latter band is substantially lower than ozonide bending modes (600 cm^{-1})[20] and probably involves mixing with the symmetric Sb–O stretching motion. A pure oxygen motion would shift to 401.3 cm^{-1} with ^{18}O, slightly more than the 407.7-cm^{-1} observed value.

(20) Spiker, R. C., Jr.; Andrews, L. *J. Chem. Phys.* **1973**, *59*, 1851, 1863.

Table V. Infrared Absorptions (cm^{-1}) Assigned to Hydroxystibine in Solid Argon

$H_2Sb^{16}OH$	$H_2Sb^{18}OH$	$D_2Sb^{16}OD$	$D_2Sb^{18}OD$	mode
3654	3643	2697	2680	O–H str
(3640)	(3626)	(2686)		site or isomer
(3625)	(3614)	(2674)	(2657)	site or isomer
1836.8	1836.8	1320.6	1320.6	$Sb–H_2$ str
1834.6	1834.6	1319.4	1219.4	site or isomer
612	582	637		site or isomer
(596)	(567)	(624)		site or isomer
(590)		608	580	site
583.5	556.5	598		Sb–O str
(574)	(548)			site or isomer

The symmetric Sb–D deformation shifts to 387 cm^{-1}, below the symmetric O–O–O mode, forcing it up to 437.9 cm^{-1} and sharing the ^{18}O shift between the two motions.

The most interesting question about the stibylene ozonide species regards its comparison to ionic ozonides $M^+O_3^-$[18-20] and primary organic ozonides.[21] The latter exhibit antisymmetric O–O–O stretching modes near 647 cm^{-1} and symmetric O–O–O bending near 409 cm^{-1}. As mentioned above, the antisymmetric O_3-subgroup absorption for $DSbO_3$ is near alkali-metal ozonide values, but the O_3-subgroup bending motion is substantially below $M^+O_3^-$ values and near the primary organic ozonide value, which indicates bonding of the terminal oxygens in the O_3 subgroup. Although the ionization energy of SbH is not known, both the appearance potential of SbH^+ from SbH_3 (9.9 ± 0.2 eV) and the ionization energy of Sb (8.64 eV) are considerably higher than alkali-metal (4–5 eV) and alkaline-earth-metal (5–6 eV) values[22] where ionic ozonides have been prepared on reagent codeposition, which makes an ionic $HSb^+O_3^-$ species unlikely. Furthermore, the light brown sample color and *complete photodissociation with 290-nm radiation* reveal an absorption spectrum different from those of the alkali-metal ozonides. Also, the observation of two well-defined H–Sb–O deformation modes indicates the well-defined structural arrangement expected for a covalently bound species. Hence, consistent with the covalent network nature of antimony oxides,[23] $HSbO_3$ likely involves primarily covalent bonding.

Group 2. The carrier of group 2 bands is difficult to identify since no deuterium counterparts were observed. The band at 654.9 cm^{-1} shows a moderate 13.8-cm^{-1} ^{18}O shift and exhibits a doublet of doublets in $^{16,18}O_3$ studies, which identifies a motion of one oxygen atom interacting slightly with a second inequivalent oxygen atom. The sharp 358-cm^{-1} band shows a 3-cm^{-1} ^{18}O shift and is appropriate for a OH torsional mode. A possible species such as H_2SbOOH would show a deuterium kinetic isotope effect that could account for no observable product. The H_2SbOH species, to be discussed below, was a major product of O_3 codeposition with SbH_3, in contrast to the corresponding D_2SbOD species. The group 2 bands are tentatively attributed to a possible H_2SbOOH molecule.

Hydroxystibine (Group 3). The absorptions of group 3 were produced in good yield by codeposition of SbH_3 and O_3 (Figure 2) but only in trace yield upon codeposition of SbD_3 and O_3 (Figure 4). Group 3 bands increased slightly with visible photolysis and markedly with UV photolysis; new absorptions were observed in three regions: just below the strong precursor Sb–H (or Sb–D) stretching modes, in the O–H (and O–D) stretching region, and near 600 cm^{-1}. The isotope shifts characterize O–H, $Sb–H_2$, and Sb–O stretching modes and identify the H_2SbOH molecular species. Similar spectra for the H_2AsOH species[5] provide support for the present identification of H_2SbOH. The several absorptions given in Table V are due to either different argon packing arrangements (sites) in the matrix or perhaps different cis or trans

(21) Kohlmiller, C. K.; Andrews, L. *J. Am. Chem. Soc.* **1981**, *103*, 2578.
(22) Rosenstock, H. M.; Draxl, K.; Steiner, B. W.; Herron, J. T. *J. Phys. Chem. Ref. Data* **1977**, *6*, suppl. 1.
(23) (a) Cotton, F. A.; Wilkinson, G. *Advanced Inorganic Chemistry*; Wiley Interscience: New York, 1962. (b) Amador, J.; Puebla, E. G.; Morge, M. A.; Rasines, I.; Valero, C. R. *Inorg. Chem.* **1988**, *27*, 1367 and references therein.

Table VI. Infrared Absorptions (cm^{-1}) Assigned to Stibine Oxide in Solid Argon

$H_3Sb^{16}O$	$H_3Sb^{18}O$	$D_3Sb^{16}O$	$D_3Sb^{18}O$	assgnt
1970	1970	1413	1413	ν_4(e) antisym Sb–H_3 str
(1962)	(1962)	(1407)	(1407)	ν_4 site
(825)[a]	(779)[a]	824.6	781.0[b]	$\nu_2(a_1)$ Sb=O str
791.8	794.2	568	568	$\nu_3(a_1)$ sym SbH_3 def
c	*c*	402.0	399.4	ν_6(e) antisym D–Sb–O def
		396.6	394.1	ν_6 site

[a] Bands obscured by strong SbH_3 absorptions; presence deduced from interaction with $\nu_3(a_1)$ and comparison to D_3SbO. [b] Weak Fermi resonance doublet component observed at 795 cm^{-1}. [c] Not observed; may be obscured by the 542-cm^{-1} product band.

isomers of H_2SbOH. Hydroxystibine is produced by direct reaction (eq 3) and by the photolysis mechanism to be discussed later.

$$SbH_3 + O_3 \longrightarrow \begin{matrix} H \\ H \end{matrix}\!\!>\!Sb-O-H + O_2 \qquad (3)$$

The O–H stretching mode and isotopic shifts for SbH_2OH are almost identical with those observed for H_2AsOH. In fact, there is a smooth trend in O–H stretching fundamentals in the series NH_2OH (3635 cm^{-1}), PH_2OH (3644 cm^{-1}), AsH_2OH (3652 cm^{-1}), and SbH_2OH (3654 cm^{-1}). This probably reflects a decrease in interaction with the more diffuse lone pair on the central element. On this basis the $-NH_2$ group appears to be more "electron donating" as the limit in this trend is OH^- (3549 cm^{-1} in solid argon).[24]

The H_2SbOH species appears to be predictable in all respects. The Sb–H/Sb–D = 1834.6/1319.4 = 1.3905 ratio is almost the same as the precursor value: 1882.2/1352.7 = 1.3914. Finally, the ^{18}O counterpart (556.5 cm^{-1}) for the Sb–O stretching mode (583.5 cm^{-1}) is just 2 cm^{-1} short of the value calculated for a diatomic Sb–O oscillator, which indicates an almost pure Sb–O stretching mode. There is, however, a 20–28-cm^{-1} blue shift on deuteriation owing to mixing of the Sb–O stretch with the Sb–D_2 bending and deformation modes expected in the high 500-cm^{-1} region.

Group 4. Reaction products that showed only a little demise on photolysis have spectra that include a broad band with structure at 1982 cm^{-1} and a feature at 740 cm^{-1} that shows a 27-cm^{-1} oxygen-18 shift. No mixed isotopic components were found, presumably due to isotopic dilution. On deuteriation, the group 4 bands were observed at 1411 and 700 cm^{-1}. This species contains $-SbH_x$ and $-SbO_y$ subgroups. It is likely that $y < 3$, since ozonides should be photosensitive. A good possibility is $x = 1$ and $y = 1$; such a tentatively identified $HSbO_2$ species would likely be analogous to stibylene ozonide.

Stibine Oxide (Group 5). The first product formed on red photolysis at the expense of the SbD_3---O_3 complex (Scheme I) was favored in SbD_3 experiments. Sharp group 5 bands appeared at 1413, 824.6, 568, and 396.6 cm^{-1} on red photolysis. These bands (or the 402.0-cm^{-1} component) were doubled with 290–1000-nm irradiation and were reduced by one-third with full arc photolysis. The key elements are the oxygen-18 shift to 781.0 cm^{-1} for the strong 824.6-cm^{-1} band in the "Sb=O" stretching region and the *absence of intermediate components* with $^{16,18}O_3$. A harmonic Sb–O calculation predicts 783.0 cm^{-1}, which falls short of the observed shift by 2.0 cm^{-1}. This requires either more than one oxygen, which cannot be the case in view of the mixed isotopic doublet, or a Fermi resonance interaction. The latter is provided by the 399.4-, 394.1-cm^{-1} fundamentals in the SbD_3 and $^{18}O_3$ experiments and a weak new band at 795 cm^{-1} probably due to its overtone. Red photolysis (630–1000 nm) first produced the 394.1-cm^{-1} band and absorption at 779.8 cm^{-1}; continued near-UV photolysis produced the 399.4-cm^{-1} counterpart and shifted the peak higher to 781.0 cm^{-1}. The 399.4-, 394.1-cm^{-1} bands are appropriate for the ν_6(e) D—Sb=O deformation mode of D_3-

Scheme I

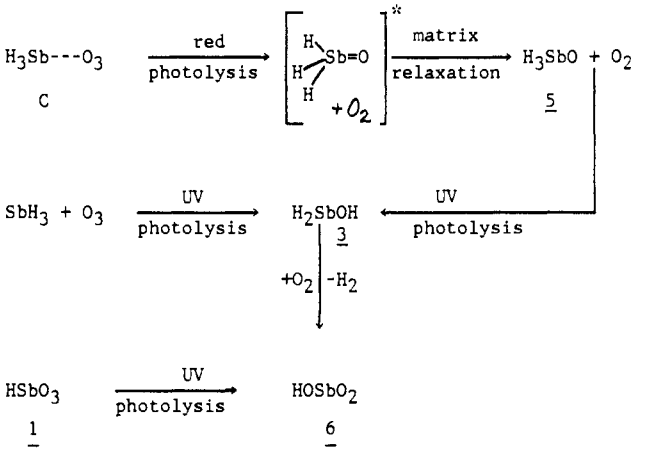

Sb=O where $2\nu_6$ at 795 cm^{-1} is in Fermi resonance with the $\nu_2(a_1)$ Sb=O stretch at 781 cm^{-1} and shifts it slightly lower than predicted from the harmonic Sb–O calculation. The strong 824.6-cm^{-1} absorption involving the stretching of a single oxygen atom near the SbO diatomic fundamental (810 cm^{-1} in the gas phase)[25] provides strong support for the identification of D_3Sb=O. Other group 5 fundamentals in the Sb–D stretching region at 1413 cm^{-1} and the symmetric SbD_3 deformation region at 568 cm^{-1} add to the evidence for the identification of D_3SbO.

The corresponding H_3Sb=O species is less stable against rearrangement to H_2SbOH with increasing photolysis energy, and most unfortunately, the two strong SbH_3 bands at 822 and 779 cm^{-1} completely mask the diagnostic Sb=O stretching modes of $H_3Sb^{16}O$ and $H_3Sb^{18}O$, respectively, which are expected to show little shift from D_3SbO on the basis of the spectra of H_3AsO and D_3AsO.[5] However, the 791.8-cm^{-1} band, which appeared on 590-nm photolysis and increased with 290- and decreased with 220-nm photolysis, is appropriate for the symmetric SbH_3 deformation of H_3SbO. Following the appearance of the ν_3 mode of D_3SbO just 9 cm^{-1} above ν_2 of SbD_3, ν_3 of H_3SbO is expected 12 cm^{-1} above ν_2 of SbH_3, as observed here. This assignment is confirmed by the blue shift of the 791.8-cm^{-1} band to 794.2 cm^{-1} with ^{18}O, which arises from interaction with the "Sb=O" stretching mode of $H_3Sb^{18}O$ expected near 780 cm^{-1} on the basis of the spectrum observed here for $D_3Sb^{18}O$.

The diagnostic "Sb=O" stretching fundamental of stibine oxide at 824 cm^{-1} is above this fundamental for trialkylstibine oxides (678 cm^{-1}) in solution.[26] A similar relationship has been found for H_3PO, H_3AsO, and their trialkyl derivatives although the difference is much greater for the stibine compounds. In view of the appearance of the diatomic group 15 oxide MO and H_3MO fundamentals[4,5] within 20 cm^{-1}, the D_3SbO and R_3SbO discrepancies imply that the R_3SbO species is associated in solution.

The effect of oxygen on the bonds involving hydrogen in the series H_3PO, H_3AsO, and H_3SbO appears to be more pronounced with antimony. The blue shift in ν_3 for the hydride compared to ν_4 for the oxide increases from 27 and 24 cm^{-1} for H_3PO and H_3AsO to 88 cm^{-1} for H_3SbO. Finally, consistent with the near-UV photolysis of stibine, stibine oxide also photodissociates with the unfiltered mercury arc.

Group 6. Weak bands in the last group were produced and increased with UV photolysis. Again, the spectrum is not complete for either the protonated or deuteriated species because product absorptions are probably masked by precursor. The absorptions given in Table VII include OH and OD stretches below those for species 3, an Sb–O stretch above species 3, a sharp 778.5-cm^{-1} absorption, and a low-frequency band at 370 cm^{-1}. Although the

(24) Suzer, S.; Andrews, L. *J. Chem. Phys.* **1988**, *88*, 916.
(25) Balfour, W. J.; Ram, R. S. *J. Mol. Spectrosc.* **1984**, *105*, 246.
(26) Chremos, G. N.; Zingaro, R. A. *J. Organomet. Chem.* **1970**, *22*, 637. Morris, W.; Zingaro, R. A.; Laane, J. *Ibid.* **1975**, *91*, 295.
(27) Fraser, M. E.; Stedman, D. H. *J. Chem. Soc., Faraday Trans. 1* **1983**, *79*, 527.

Table VII. Infrared Absorptions (cm^{-1}) Assigned to Metaantimonic Acid, $HOSbO_2$, in Solid Argon

SbH_3		SbD_3		
^{16}O	^{18}O	^{16}O	^{18}O	assgnt
3604	3593	2658	2642	ν(O–H) str
3575		2644	2627	site
a	737.6	778.5	736.5	$\nu_{sym}(SbO_2)$ str
635	604	*b*	*a*	ν(Sb–O) str
370	369	276	272	τ(O–H) torsion

[a] Masked by precursor. [b] One of the bands between 647 and 598 cm^{-1} could be the counterpart of the 635-cm^{-1} band.

spectrum is incomplete, some conclusions can be drawn from the available data. The sharp 778.5-cm^{-1} band for the deuteriated species has an oxygen-18 counterpart at 736.5 cm^{-1} *and* a stronger 759.1-cm^{-1} intermediate component with $^{16,18}O_3$; this evidence identifies a vibration involving primarily *two equivalent oxygen atoms*. The ^{18}O shift is appropriate for a symmetric Sb–O_2 stretching mode. Only the ^{18}O counterpart was observed for the protonated compound (owing to SbH_3 absorption), and the 1.1-cm^{-1} shift shows that this species contains hydrogen, consistent with observation of an O–H stretching mode. The strong sharp 635-cm^{-1} band is due to an Sb–O vibration based on ±1-cm^{-1} agreement between calculated and observed oxygen-18 counterparts. The 370-cm^{-1} band shows D and ^{18}O shifts appropriate for an –OH torsional motion. Accordingly, the group 6 bands are best assigned to $HOSbO_2$. This molecular species is analogous to $HOAsO_2$ and $HOPO_2$, which increased on full arc photolysis in similar AsH_3 and PH_3 experiments.[4,5]

Photolysis Mechanism. The mechanism of photolysis has been outlined in Scheme I, and a few points will be emphasized here. The favorable red photolysis of ozone in the complex is due to a specific interaction with stibine and the ability of SbH_3 to form a strong bond to oxygen. Such red photolysis has been observed for PH_3, AsH_3, and PCl_3 complexes with ozone.[4,5,10] A key element for the stabilization of H_3SbO is matrix relaxation of the excited $[H_3SbO]^*$ species formed by the initial O atom addition.

Ultraviolet photolysis decreased H_3SbO, destroyed $HSbO_3$, produced $HOSbO_2$, and markedly increased H_2SbOH. A major contributor to the last occurrence is the photolysis of isolated ozone and the insertion of $O(^1D)$ into an Sb–H bond to give H_2SbOH. The photolysis of $HSbO_3$ probably gives HSbO and O_2, which quickly react to produce $HOSbO_2$; the analogous latter reaction was observed for the PH_3/O_3 system.[4]

Reactivity Trends. Matrix codeposition of NH_3, PH_3, AsH_3, and SbH_3 samples diluted in argon with ozone diluted in argon provides a basis for comparison of the relative reactivities of the group 15 hydrides. No codeposition reaction products were observed for NH_3 and PH_3; however, H_2AsOH was observed with AsH_3, and H_2SbOH was produced with SbH_3. In addition, the $HSbO_3$ ozonide species was observed for the SbH_3 reaction and no evidence for such a species was found with AsH_3. Clearly the group 15 hydride reactivity with O_3 increases on going down the periodic table. A gas-phase investigation of chemiluminescent reactions in these systems[26] underscores their high reactivities but does not provide information on the relative reactivities of the hydrides.

Although H_2AsOH and H_2SbOH were codeposition reaction products, photolysis was required to produce a significant yield of the deuteriated species. Even on photolysis, the yields of H_2AsOH and H_2SbOH were larger relative to those of H_3AsO and H_3SbO than were the yields of D_2AsOD and D_2SbOD relative to those of D_3AsO and D_3SbO. This indicates a significant kinetic isotope effect for the insertion reaction and rearrangement of the deuteriated species. Finally, the yield of $DSbO_3$ was larger than the yield of $HSbO_3$ on the basis of band intensities. Since the ozonides are produced by an addition reaction followed by H_2 (or D_2) elimination, the greater yield of $DSbO_3$ points to its greater stability. For a hydride of limited stability, the added stability arising from lower zero-point energy for deuterium is more significant.

Finally, the classical trend of decreasing stability of the higher (V) oxidation state on going down a family in the periodic table is illustrated here. The compounds involving the V oxidation state, H_3SbO and $HOSbO_2$, are produced here in much lower yield relative to their V oxidation state analogues in AsH_3 and PH_3 investigations and relative to the lower (III) oxidation state species H_2SbOH.

Conclusions

Stibine and ozone were codeposited with excess argon at 12 K. Infrared spectra revealed major reaction products, which were identified as stibylene ozonide, $HSbO_3$, and hydroxystibine, H_2SbOH, on the basis of isotopic substitution (SbH_3, SbD_3, $^{16}O_3$, $^{18}O_3$, $^{16,18}O_3$). Deuterium substitution gave more $DSbO_3$ and much less D_2SbOD upon codeposition. There appears to be a significant kinetic isotope effect for O-insertion reactions. Red photolysis of stibine/ozone samples gave new bands identified as stibine oxide, H_3SbO; the deuterium counterpart D_3SbO was a favored product with SbD_3. Ultraviolet photolysis destroyed $HSbO_3$, decreased H_3SbO, increased H_2SbOH, and produced weak new bands attributed to $HOSbO_2$. Ultraviolet photolysis of separate SbH_3 and SbD_3 samples gave new bands for the SbH_2 and SbD_2 free radicals.

The SbH_3/O_3 matrix studies gave species similar to those from experiments with PH_3 and AsH_3, including H_2SbOH and H_3SbO. Expected differences are decreasing stability of V oxidation state species with SbH_3 and increased reactivity of SbH_3 with O_3 to give a new type of ozonide species, $HSbO_3$, not observed with the lighter group 15 hydrides.

Acknowledgment. We gratefully acknowledge financial support from NSF Grant CHE 85-16611, sabbatical support for B.W.M. from Randolph-Macon College, the use of R. N. Grimes' laboratory to synthesize stibine, and the assistance of Z. Mielke with several experiments.

Registry No. SbH_3, 7803-52-3; SbD_3, 13537-04-7; O_3, 10028-15-6; $HSb^{16}O_3$, 117860-61-4; $HSb^{18}O_3$, 117860-62-5; $DSb^{16}O_3$, 117860-63-6; $DSb^{18}O_3$, 117860-64-7; $H_2Sb^{16}OH$, 14798-33-5; $H_2Sb^{18}OH$, 117860-65-8; $D_2Sb^{16}OH$, 117860-66-9; $D_2Sb^{18}OH$, 117860-67-0; $H_3Sb^{16}O$, 31219-54-2; $H_3Sb^{18}O$, 117860-68-1; $D_3Sb^{16}O$, 117860-69-2; $D_3Sb^{18}O$, 117860-70-5; $HOSbO_2$, 13473-74-0; Ar, 7440-37-1; SbH_2, 20346-77-4; SbD_2, 117860-72-7; ^{16}O, 17778-80-2; ^{18}O, 14797-71-8; D_2, 7782-39-0.